

TECHNICAL UNIVERSITY OF CRETE

BACHELOR THESIS

**Dynamic Analysis of a Friction
Pendulum Isolation System (FPS) under
earthquake excitation**

Author:

Antonios P. Lousidis

Supervisor:

Dr. Georgios E. Stavroulakis

*A thesis submitted in fulfilment of the requirements
for the degree of Bachelor of Engineering*

in the

Institute of Computational Mechanics and Optimization
Department of Production Engineering and Management

September 2015

Declaration of Authorship

I, Antonios P. LOUSIDIS, declare that this thesis titled, 'Dynamic Analysis of a Friction Pendulum Isolation System (FPS) under earthquake excitation' and the work presented in it are my own. I confirm that:

- This work was done wholly or mainly while in candidature for a research degree at this University.
- Where any part of this thesis has previously been submitted for a degree or any other qualification at this University or any other institution, this has been clearly stated.
- Where I have consulted the published work of others, this is always clearly attributed.
- Where I have quoted from the work of others, the source is always given. With the exception of such quotations, this thesis is entirely my own work.
- I have acknowledged all main sources of help.
- Where the thesis is based on work done by myself jointly with others, I have made clear exactly what was done by others and what I have contributed myself.

Signed:

Date:

TECHNICAL UNIVERSITY OF CRETE

Abstract

Faculty of Engineering

Department of Production Engineering and Management

Bachelor of Engineering

Dynamic Analysis of a Friction Pendulum Isolation System (FPS) under earthquake excitation

by Antonios P. LOUSIDIS

Base isolation systems have become a significant element of a structure to enhance reliability during an earthquake excitation. It is an acknowledged method to reduce the transmission of ground acceleration into the structural system, by increasing the natural period of the structure. The need for a base isolation system may arise in an area of high seismic activity, if increased safety and post-earthquake operability is required. One kind of methods of base isolation is the Friction Pendulum Isolation System (FPS). This study centres on the development of a dynamic response analysis of a structural scheme isolated with frictional pendulum system. Results of the mathematical model developed are presented for two structure examples. The first one deals with the seismic response of a conventional fix-based rigid superstructure and the second one presents the earthquake response of a base isolated building supported on (FPS) isolators. Both structural schemes subjected on the Kobe earthquake and a numerical simulation is performed in order to demonstrate the effectiveness and applicability of the (FPS) system.

Acknowledgements

This research has been conducted as a bachelor thesis of The Technical University of Crete, department of Production Engineering and Management. Part of this research has been performed during my internship at Stavros Niarchos Foundation Cultural Center (SNFCC) Worksite which is located in Athens, Greece.

First of all, I would like to express my sincere gratitude to my supervisor Prof. dr. Georgios Stavroulakis for his support and advice of my study and related research. His guidance helped me in all the time of research and writing of this thesis. My sincere thanks also goes to Mr. Manos Vrailas and GEK TERNA S.A. who provided me an opportunity to join their team as intern, and who gave access to SNFCC work site facilities.

Last but not least, I would like to thank my family for their unconditional support and ever-lasting faith in me.

Contents

Declaration of Authorship	i
Abstract	ii
Acknowledgements	iii
List of Figures	vi
List of Tables	viii
Abbreviations	ix
Physical Constants	x
Symbols	xi
1 Introduction	1
2 Literature review	2
2.1 Base isolation: An Earthquake resistant Approach	2
2.2 History of Base isolation	2
2.3 Applications of Base Isolation Worldwide	4
2.3.1 Base isolation in United States	4
2.3.2 Base isolation in Europe	5
2.3.3 Base isolation in Japan	5
2.4 Applications of Base Isolation in Greece	6
2.4.1 Stavros Niarchos Foundation Cultural Center (SNFCC)	6
2.5 Types of Base Isolation	8
2.5.1 Low-Damping Natural and Synthetic Rubber Bearings	8
2.5.2 Lead-Plug Bearings	8
2.5.3 High-Damping Natural Rubber Systems (HDNR)	8
2.5.4 The Friction Pendulum Isolation System (FPS)	9
2.5.5 Installation of FPS Bearings according to the manufactures guide .	12
2.5.5.1 Acceptance of the Pendulum Bearings	15
2.5.5.2 Storage	15

2.5.5.3	Placing and Adjusting	15
2.5.5.4	Grouting (Mortar Bed)	16
2.5.5.5	Construction of Mortar Bed	16
2.5.5.6	Concrete Superstructure	18
3	Friction Models	19
3.1	Introduction	19
3.2	The phenomenon of Friction	19
3.3	Classical Static Models	21
3.3.1	Coulomb Friction	21
3.3.2	Coulomb plus viscous friction	21
3.3.3	Stiction plus Coulomb plus Viscous Friction	22
3.3.4	Non-linearity: Stribeck effect	23
3.4	Dynamic Models	23
3.4.1	The Dahl Model	23
3.4.2	The Bristle Model	25
3.4.3	The LuGre Model	26
3.4.4	The Leuven Model	27
3.5	Friction Damping	28
4	Non Linear Dynamic Analysis Procedure	30
4.1	Modelling and Analysis Details	30
4.2	The Concept of Base Isolation	33
4.2.1	Effectiveness of base isolation	33
5	Results	35
6	Conclusions	38
6.1	Conclusions	38
A	MATLAB Simulink Models	40
B	State Space Formulation	41
	Bibliography	44

List of Figures

2.1	Functions of a Bearing	3
2.2	Base Isolation by wooden logs	4
2.3	Stavros Niarchos Foundation Cultural Center (SNFCC)	6
2.4	Stavros Niarchos Foundation Cultural Center (SNFCC) 3D model	7
2.5	Positions of the Seismic Bearings-Library Building	7
2.6	Lead-Rubber Bearing Isolator	9
2.7	Hysteretic behaviour of high damping rubber isolation systems	10
2.8	Frictional Properties of FPS Bearings	13
2.9	Cross Sectional View of FPS Bearings	13
2.10	Friction Pendulum Sliding Isolator	14
2.11	a) The mathematical model of the pendulum in the Equilibrium Phase b) Dynamical Characteristics of the FPS	14
2.12	Construction and Installation of the Mortar Bed	17
2.13	Construction and Installation of the Mortar Bed using the free flow mortar	17
3.1	Simplification of the friction Phenomena	20
3.2	Coulomb Friction	21
3.3	Coulomb plus Viscous Friction	22
3.4	Stiction plus Coulomb plus Viscous Friction	22
3.5	Stribeck Effect	23
3.6	Friction Force vs. Displacement for the Dahl Model	24
3.7	Asperities between two surfaces in contact	25
3.8	Evolutionary variable that corresponds to bristle deflection	26
3.9	Coulomb damping Force vs Displacement	28
3.10	Structural damping Force vs Displacement	28
4.1	Model for dynamic analysis	31
4.2	System modelled in Matlab	31
4.3	Response spectrum for ground motion recorder on Sep 19,1985 at SCT site on Mexico City and spectral ordinates for fixed-base and isolated building	34
4.4	Natural Vibration Models	34
5.1	Acceleration of Top Floor VS Time	35
5.2	Displacement of Top Floor VS Time	36
5.3	Upper and Lower Slab Accelerations VS Time	36
5.4	Behaviour of Friction Forces (F_r) vs Displacement	37
A.1	Uncontrolled Simulink Model	40

A.2	Controlled Simulink Model with the Inclusion of Friction	40
B.1	SDOF System	41

List of Tables

Abbreviations

FPS	F riction P endulum S ystem
BI	B ase I solation
LRB	L aminated R ubber B earing
HDRB	H igh D ensity R ubber B earings
PTFE	P olytetrafluoroethylene

Physical Constants

Acceleration of Gravity $g = 9.81 \text{ m/s}^2$ (exact)

Symbols

F	Lateral Force	Nt
u	Bearing Displacement	m
\dot{u}	Bearing Velocity	m/s
R	Radius of Curvature	m
μ	Coefficient of sliding friction	
f_{max}	Value of coefficient of friction at high velocity of sliding	
f_{min}	Value of coefficient of friction at very low sliding velocity	
a	Parameter that controls the variation of friction with the velocity of sliding	
ω	Angular frequency	rads ⁻¹

Dedicated to my Parents...

Chapter 1

Introduction

Although isolation as a method for mounting mechanical equipment has been employed for many years ago, the idea of isolating civil structures such as bridges, buildings etc from the damaging effects of an earthquake has been introduced recently. During a seismic event the ground motion interacts with the structure at the foundation level and dissipates energy in the entire structure. Therefore it is of great importance to isolate the structure at its base in order to prevent the earthquake-induced forces in a structure and minimize damage caused by lateral displacements. There are three types of base isolation mechanism that are commonly used in practice. High Density Rubber Bearings (HDRB) are comprised by specially formulated rubber disks that serve as damping agent. Laminated Rubber Bearings (LRB), which have similar characteristics to the (HDRB) however, they use different type of rubber for damping agent. The third type of base isolation mechanism is the Friction Pendulum System (FPS). Friction Pendulum Bearings consist of three basic elements: A primary curved sliding surface, whose radius of curvature determines the oscillation period of the isolator, a steel rocking element equipped with a sliding material usually Teflon, which slides along the primary curved sliding surface and a fixed steel plate designed to allow the rotations induced by the horizontal displacement of the isolators. The size of the primary sliding surface depends on the maximum desired displacement and the damping is selected by choosing the the appropriate friction coefficient. In this thesis a structural control scheme will be proposed in order to reduce the response of a building under earthquake excitation. The structure will be isolated at its base using the Friction Pendulum Isolation System (FPS).

Chapter 2

Literature review

2.1 Base isolation: An Earthquake resistant Approach

The term isolation refers to the degree of interaction between objects. An object is said to be isolated if it has little or no interaction with other objects. By isolating an object we provide an interface between the object and its neighbours that minimizes interaction. This definition applies to many other examples such as the isolation system in Thermodynamics. A very common application is the design of isolation systems for vibrating machinery. Another application is the concept of protecting a structure from an earthquake by introducing some type of devices that isolate the structure at its base from ground motion. These devices are called base isolation systems and many types of them have been proposed in the past. Base isolation systems for Buildings has been introduced to isolate the structure from the potential damages induced by ground motion. The mechanism of base isolator increases the natural period of the structure and simultaneously decreases its acceleration to earthquake motion. It is based on the structural bearing technology, which is the connection element between the superstructure and substructure and allows horizontal displacement, rotation and movement.

2.2 History of Base isolation

The first base isolation device has been installed in the Tokoyo Imperial Hotel in early 1900's and the first material that has been used was the Lead Rubber Bearing (LBR), which provided high flexibility and damping. After 80 years the High Damping Rubber has been launched and used in structures in US. The only drawback was that these devices had no restoring mechanism and they dislocate after a ground motion. Since 1840's the

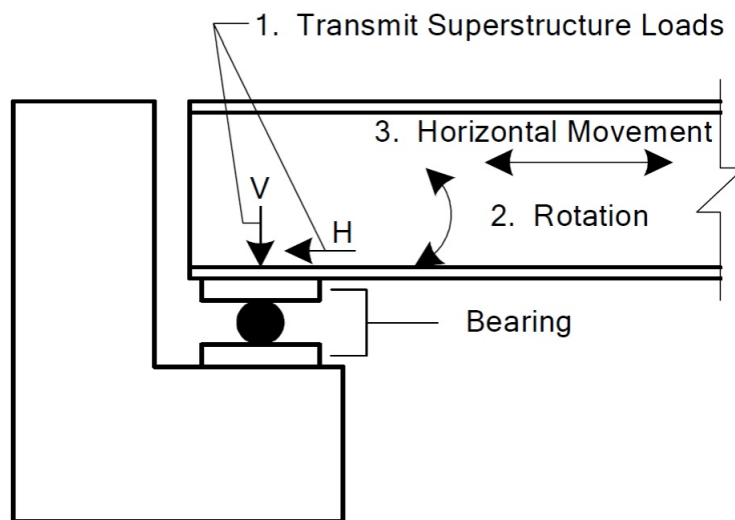


FIGURE 2.1: Functions of a Bearing.

natural rubber has been used for base isolation. The material that has been developed was the synthetic rubber or polytetrafluoroethylene (PTFE) for more than 50 years. After a period of time the Lead Rubber Bearing technology (LBR) has been launched and used especially in bridges, providing an increase of 7% in stiffness after 37 years from installation, with oxidation restriction to 10mm to 20mm.[1] In 1891 a Japanese person introduced a method for seismic isolation by proposing a base isolated structure with timber logs placed in several layers in the longitudinal and transverse direction [2] as shown in Figure 2.2. In 1906, Jacob Bechtold, a German Engineer applied a patent in which he introduced a structure on a rigid plate which supported on spherical mechanisms of a hard material.[3]. The first rubber isolation system installed in an elementary school in Skopje, Yugoslavia in 1969, The Pestalozzi School which was a three-storey concrete building designed and built by Swiss engineers. Unlike the rubber bearing technology that is widely known in the engineering community, these bearings are unreinforced so that the weight of the building causes them to bulge sideways. There have been used special glass blocks acting as seismic fuzes are intended to break when the ground shaking load exceeded a certain threshold. This bearing technology was replaced by the reinforcing rubber blocks with steel plates.[4]

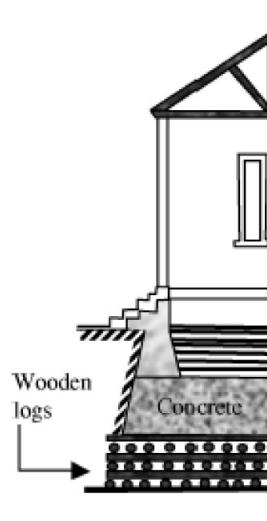


FIGURE 2.2: Base Isolation by wooden logs [2].

2.3 Applications of Base Isolation Worldwide

2.3.1 Base isolation in United States

The first base isolated building in the US was the Foothill Communities Law and Justice Center (FCLJC), legal services center for the County of San Bernardino, located in the city of Rancho Cucamonga, about 97 km away of Los Angeles. It was also the first building that made use of isolations bearings made from high-damping natural rubber. The county of San Fault which is located about 20 km away from the (FCLJC) building was very seismically active, because of generating very large earthquakes in its southern branch. The four-story building was designed to withstand an 8.3 magnitude earthquake supported by 98 base isolation high damping bearings. The building began to being constructed in the early 80's and was completed in 1985. It costed around \$38 million. Another interesting example was the Los Angeles City Hall. A 28th storey steel frame building with a total floor area close to $83.000 m^2$. The structure which was supported by steel cross bracing, reinforced concrete walls and masonry infill perimeter walls. The building was hit by the North bridge earthquake in 1994. Severe damages have been inspected on the twenty-fifth and twenty-sixth floors which are the more elastic stories. The Los Angeles City Hall building was supported by 475 high-damping rubber isolators at its base combined with 60 sliders. Also it is to be installed about 52 mechanical viscous dampers at the foundation level and 12 viscous dampers will be placed between the twenty-fourth and twenty-sixth floors in order to control the lateral displacements at these storey levels. A recent application of Friction Pendulum System (FPS) base isolation is the seismic retrofit of the U.S Court of Appeals building in San

Francisco. It is a five storey building with a total area of $32.516 m^2$ and was built around 1900's. It is placed by steel gravity frame with unreinforced granite and brick masonry walls. The FPS base isolators were installed in the undercroft level of the structure with new concrete columns and a new rigid diaphragm system above the isolation level [4].

2.3.2 Base isolation in Europe

Base isolation is studied actively also in Europe and has been applied in many structures under the guardianship of the National Working Group of Seismic Isolation [Gruppo de Lavoro Isolamento Sismico (GLIS)]. Mainly in Italy several buildings have been built using base isolation. The new administration Center of the National Telephone Company (CIP) is complex of five seven-story structures in the port of Italy, Ancona that have been seismically isolated. A second base isolated building has been constructed in Ancona for the Ministry of Defence. Also the church of St.Peter has been retrofitted using high-damping rubber bearings.

2.3.3 Base isolation in Japan

Due to high seismic activity in Japan, Japanese structural Engineers generally design more earthquake-resistant structures than U.S or European Engineers and are willing to consider more costly designs. There are companies that introduce different kinds of mechanisms for the seismic protection of buildings and consequently are highly developed in terms of seismic isolation technology. The first base-isolated building in Japan completed in 1986. Five years later, the use of seismic isolation increased to 10 buildings per year. Due to the economic crisis that troubled Japan, the rate of construction of base isolated buildings slowed down to around 4 or 5 structures per year. At the time of the Kobe earthquake happened in 1995 the number of isolated structures rose to around 80. A very large base-isolated building in Japan is the West Japan Postal Computer Center (JPCC) located in in Sanda, a region around 30 km far from the epicenter of the 1995 Kobe earthquake. It is a six-story building with a total area of $47.000m^2$ supported on 120 elastomeric base isolators. This building has an isolated period of 3.9 sec and no damage has been reported after the earthquake.

2.4 Applications of Base Isolation in Greece

2.4.1 Stavros Niarchos Foundation Cultural Center (SNFCC)

The inspiration of this thesis came during my internship at the joint venture Impregilo-GEK-TERNA S.A. These two construction companies are the main contractors of the Stavros Niarchos Foundation Cultural Center (SNFCC) project. The (SNFCC) project site (Figure 2.3) is located 4.5 km south of the center of Athens, on the edge of Faliro Bay and is designed as a multifunctional arts, education and entertainment complex. It will include within its 170.000 m^2 park, new state of the art facilities for the Greek National Opera of Greece and National Library of Greece. The buildings were designed by Renzo Piano, the internationally acclaimed architect for the Centre Georges Pompidou in Paris. The project budget is \$ 706.78 millions and is the largest construction project Greece. In order to ensure that the buildings of the National Library of Greece and the Greek National Opera will survive a serious earthquake, these two structures are built on (FPS) base isolators specifically on RESTON PENDULUM Curved Surface Sliders. This type of base isolation bearing is in terms of technology very advanced. It is based on the physical model of a pendulum and during an earthquake event it can achieve the re-centering which is so important for the supported structure. The two structures are supported on 323 seismic isolators that can allow movements up to 350 mm and carry loads of up to 70.000 kN. Figure 2.5 shows the positions of the 151 bearings that support the Library building.



FIGURE 2.3: Stavros Niarchos Foundation Cultural Center (SNFCC).

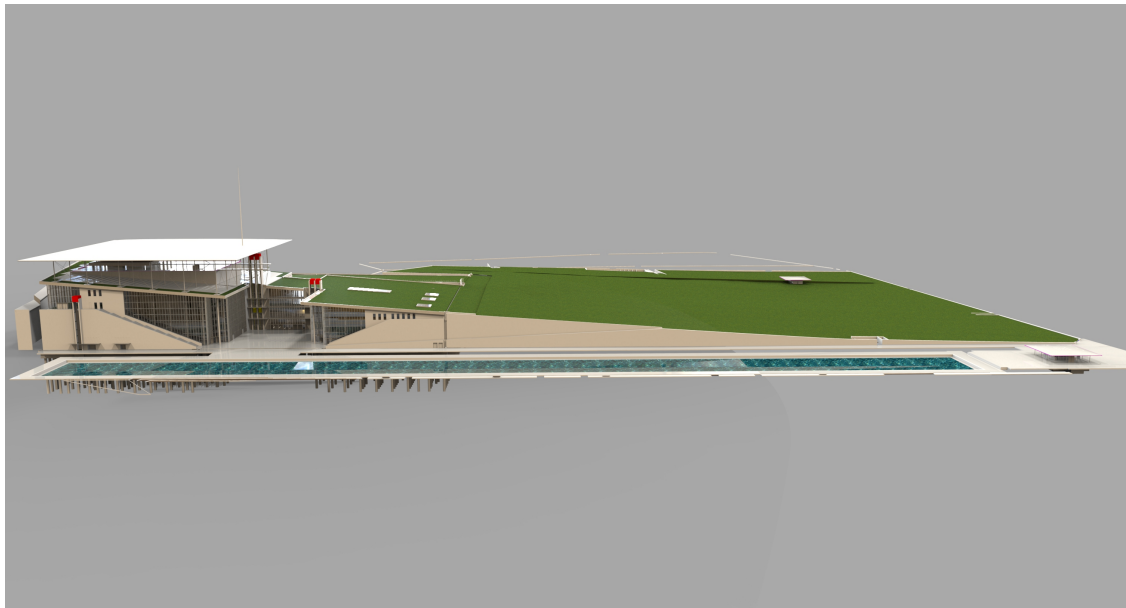


FIGURE 2.4: Stavros Niarchos Foundation Cultural Center (SNFCC) 3D Model.

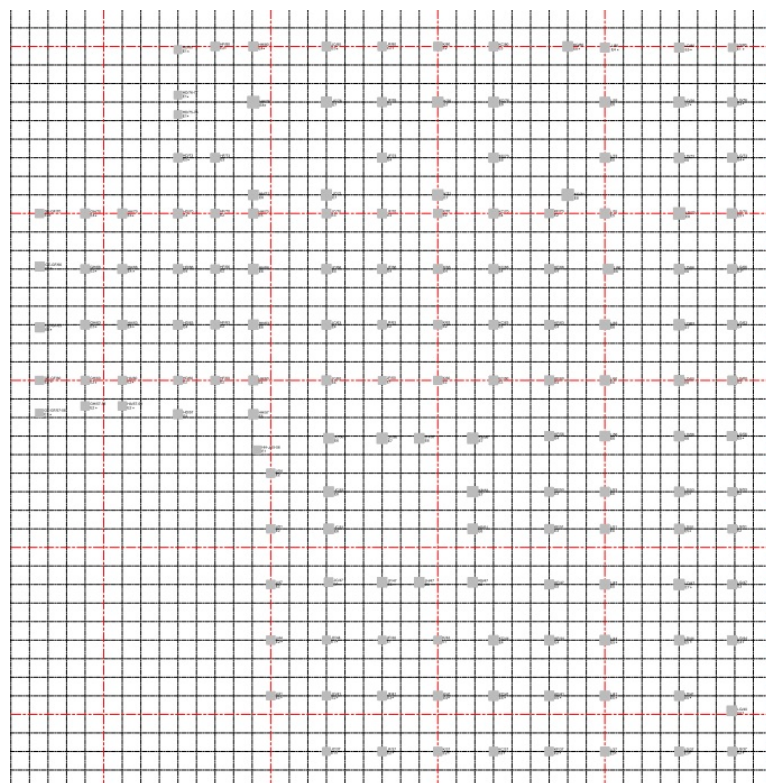


FIGURE 2.5: Positions of the Seismic Bearings-Library Building.

2.5 Types of Base Isolation

2.5.1 Low-Damping Natural and Synthetic Rubber Bearings

This type of seismic isolation has been applied mainly in Japan in conjunction with supplementary damping devices such as viscous dampers, sliding mechanisms and so on. These isolators have two thick steel endplates and many thin steel shims. The rubber is vulcanized and bonded to the steel in a single operation under heat and pressure in a mold. The steel shims prevent bulging of the rubber and provide a high vertical stiffness. The advantages this kind of seismic isolation has are many: First of all, they are simple to manufacture (the compounding and bonding process to steel is well known), easy to model and their mechanical response is unaffected by rate, temperature, history or aging [4]. The only disadvantage is that an extra damping system is needed. Below a variant of this approach, the lead-plug bearing will be discussed, which is the most frequently used isolation system.

2.5.2 Lead-Plug Bearings

The lead-plug bearing technology was invented in New Zealand in 1975 and has been used mainly in New Zealand, Japan and United States. Lead-Plug bearings are laminated rubber bearings similar to low-damping rubber bearings but contain one or more lead plugs that are inserted into holes. The steel plates in the bearing force the lead plug to deform in shear. The lead in the bearing deforms physically at a flow stress of around 10 MPa, providing the bearing with a bilinear response. It is very important, the lead to be fit tightly in the elastomeric part of the bearing, and this is achieved by developing the lead plug few millimetres larger than the hole and forcing it in. Before the installation of the lead rubber bearing, it is necessary to specify the displacement at which a specific damping value is required.

2.5.3 High-Damping Natural Rubber Systems (HDNR)

Malaysian Rubber Producers' Research Association (MRPRA) based in United Kingdom developed a natural rubber compound with enough damping in order to reduce the need for extra damping devices during seismic isolation. By adding extrafine carbon black, resins and other proprietary fillers, damping is increased to levels between 10 and 20% at 100% shear strains and a shear modulus around 0.34 MPa at lower levels of hardness and 1.40 MPa at higher levels. This specific material is non linear at shear strains less than 20% and is focused more on higher stiffness and damping in order to minimize

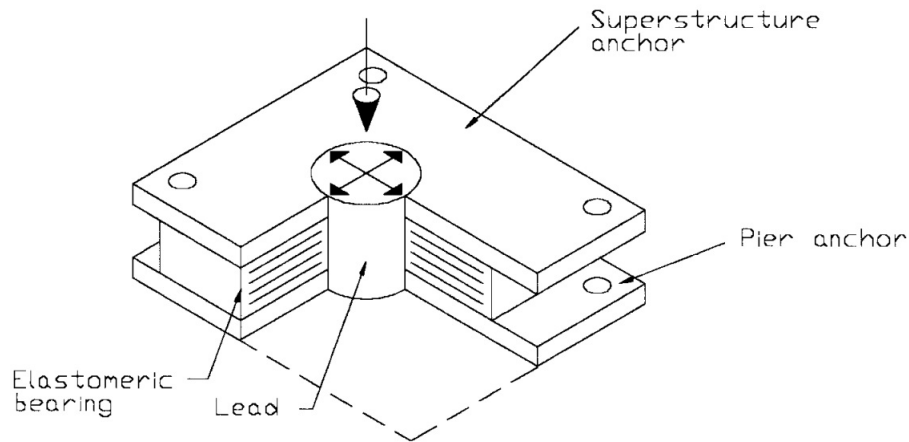


FIGURE 2.6: Lead-Rubber Bearing Isolator.

seismic and wind loads. Between 20 and 120% of shear strain the modulus is constant and low and at large strains it increases because of a strain crystallization process in the rubber which can increase energy dissipation. At large strains, the increase in stiffness and damping can develop a stiff system for small input and a linear and flexible at design level input. It can also limit displacements under unexpected input levels that exceed design levels.

The Damping in seismic isolation systems is between the viscous and hysteric phase. In a clear linear viscous element the dissipation of energy is quadratic in the displacement unlike in a hysteric system it is linear. Results from tests from many kinds of rubber isolators demonstrate that the energy dissipation per cycle is proportional to the displacement around the value of power 1.5. This characteristic can be exploited to model effectively the bearing response, which combines linear viscous and elastic-plastic elements (Fig 2.7).

Another very important characteristic of high damping rubber isolators is that they provide vibration reduction by filtering high frequency vibration caused by underground traffic. [4]

2.5.4 The Friction Pendulum Isolation System (FPS)

Another seismic isolation method is the Friction Pendulum Isolation system (FPS) that has been extensively used (Fig 2.9). The sliding and recentering mechanisms take place in one unit and the sliding surface takes a concave spherical phase.[5] The functional principle of the friction pendulum bearing is simple: a spherical bearing surface which realizes a pendulum system whose fundamental period is related essentially to the length of the pendulum, otherwise the radius of curvature of the spherical sliding surface, and

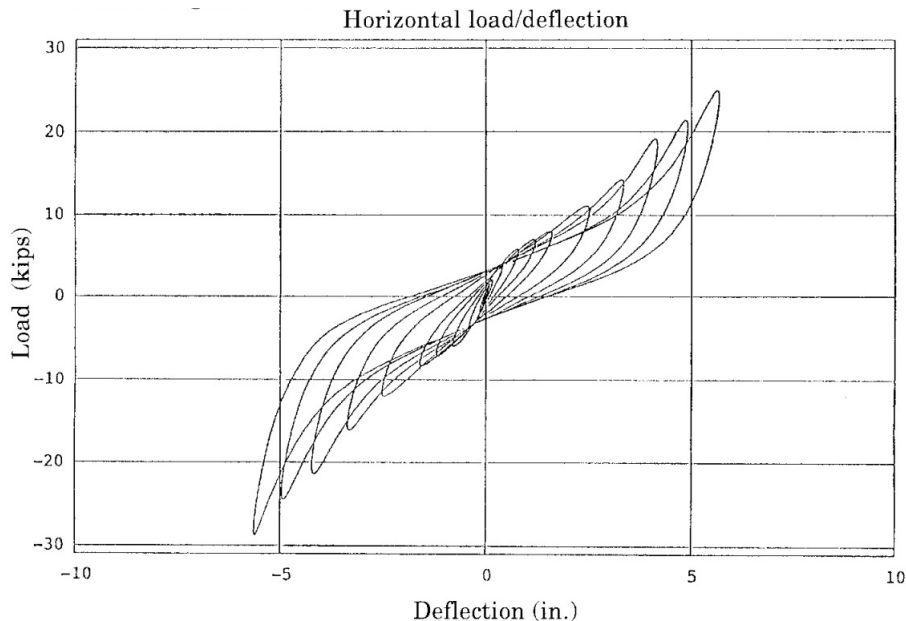


FIGURE 2.7: Hysteretic behaviour of high damping rubber isolation systems

therefore the dynamic response of these bearings is strictly related to the friction behaviour. The articulated slider is based with a high bearing-capacity composite material. The bearing is sealed and installed with the sliding surface down, so that the contamination of the sliding interface is avoided. The FPS bearing acts as a fuse, which is activated only when the shear force overcomes the static friction force. During the motion, the articulated slider moves along the concave spherical surface, causing the supported mass to rise with motions which are the same of a simple pendulum. The kinematics and operation of the bearing is the same whether the concave is facing up or down. Essentially, geometry and gravity achieve the desired seismic-isolation results. During the rise along the spherical surface the bearing develops a lateral resisting force equal to the combination of the mobilized frictional force and the gravity-induced restoring force. The lateral force is equal to:

$$F = (W/R)u + \mu W \operatorname{sgn}(\dot{u}) \quad (2.1)$$

Equation (2.1) shows that the lateral force is directly proportional to the supported weight. The center of stiffness and lateral resistance of the bearing is directly connected with the center of mass of the supported structure and compensates for mass eccentricities. This property minimizes the torsional motion of the supported structure, which can cause damage to the structure. When the threshold of static friction is exceeded the structure responds at its isolated period with the dynamic response and damping controlled by the seismic isolator bearing. Moreover the natural period of the isolated

the FPS isolated structure is independent of the weight of the building and is given by the equation (2.2)

$$T_b = 2\pi(R/g)^{1/2} \quad (2.2)$$

The coefficient of sliding friction of the FPS bearing is given by the equation (2.3):

$$\mu = f_{max} - (f_{max} - f_{min}) \exp(-\xi|\dot{D}|) \quad (2.3)$$

where f_{max} is the value of coefficient of friction at high velocity of sliding; f_{min} is the value at low sliding velocity; ξ is the parameter that controls the variation of the coefficient of friction with the velocity of sliding. Typically, f_{max} is dependent on the bearing pressure and is attained at velocities that exceed about 50 mm/s (The parameter ξ equals to 0.1 to 0.2 s/mm). And \dot{D} represents the velocity of the bearing movement.

The post yield stiffness is represented by the equation 2.4 as shown below.

$$k_p = \frac{P_c}{R} \quad (2.4)$$

where R represents the radius of curvature of the sliding surface. Test results indicate that the elastic stiffness of the friction pendulum bearing, k_e is normally 100 times larger than the postyield stiffness, k_p . [6] Accordingly, the yield displacement, D_y , is shown in the equation below:

$$D_y = \frac{Q}{k_e - k_p} \approx \frac{Q}{100k_p} = \frac{\mu_s P_c}{100 \frac{P_c}{R}} = \frac{\mu_s R}{100} \quad (2.5)$$

Essentially equation 2.5 implies that the yield displacement, D_y is a very small value nearly $2.54mm$. The effective stiffness of the friction Pendulum Bearing at the design displacement, D_D can be written as follows:

$$k_{eff} = k_p + \frac{Q}{D} = P_c \left(\frac{1}{R} + \frac{\mu_s}{D_D} \right) \quad (2.6)$$

Since the yield displacement, D_y , is much smaller than the design displacement, D_D the hysteresis loop area of the friction pendulum bearing can be simplified and is approximately estimated in the equation 2.7[6]

$$E_D = 4Q(D_D - D_y) \approx 4QD_D = 4\mu_s P_c D \quad (2.7)$$

Finally by substituting Equations 2.6 and 2.7 into the following equation (2.8):

$$\beta_{eff} = \frac{4Q(D - D_y)}{2\pi k_{eff} D^2} = \frac{2Q(D - D_y)}{\pi k_{eff} D^2} \quad (2.8)$$

The effective damping of the friction pendulum system is expressed as in the equation 2.9:

$$\beta_{eff} = \frac{E_D}{2\pi k_{eff} D_D^2} = \frac{4\mu_s P_c D_D}{2\pi P_c (1/R + \mu_s/D_D) D_D^2} = \frac{2\mu_s}{\pi(D_D/R + \mu_s)} \quad (2.9)$$

Figure (2.8) presents the values of coefficients of friction f_{min} , f_{max} and μ_B which is the breakaway or static value of FPS bearings as measured in four different test programs. Essentially in the FPS seismic isolation bearings the static friction is less than the value at high velocity of sliding, the f_{max} . The controlling value f_{max} has values between about 0.12 and 0.05, depending on the bearing pressure. The tests in the figure (2.8) extend over a range of bearing pressure of about 17 MPa to 275 Mpa. The polytetrafluoroethylene (PTFE) composite which is used in the FPS bearing technology is rated to pressures of about 300 MPa and has an ultimate capacity of over 415 MPa.

Very often vertical ground accelerations and overturning moments cause fluctuations in the axial load carried by the bearings. The effect of varying axial load can affect first the mechanical properties of the bearing by increasing the stiffness and friction force and second the design forces for the bearings and foundation of the structure. Under extreme earthquake conditions uplift may occur, which needs to be evaluated.

In particular the FPS seismic isolator is constituted by a slider that oscillates around the surface of a concave spherical surface whose radius is equivalent to the pendulum length as shown in Fig 2.9 and 2.10.

2.5.5 Installation of FPS Bearings according to the manufactures guide

It is of great importance the Friction Pendulum Bearing or the VFPI bearing to be installed correctly in order to function efficiently. Therefore it is recommended to install

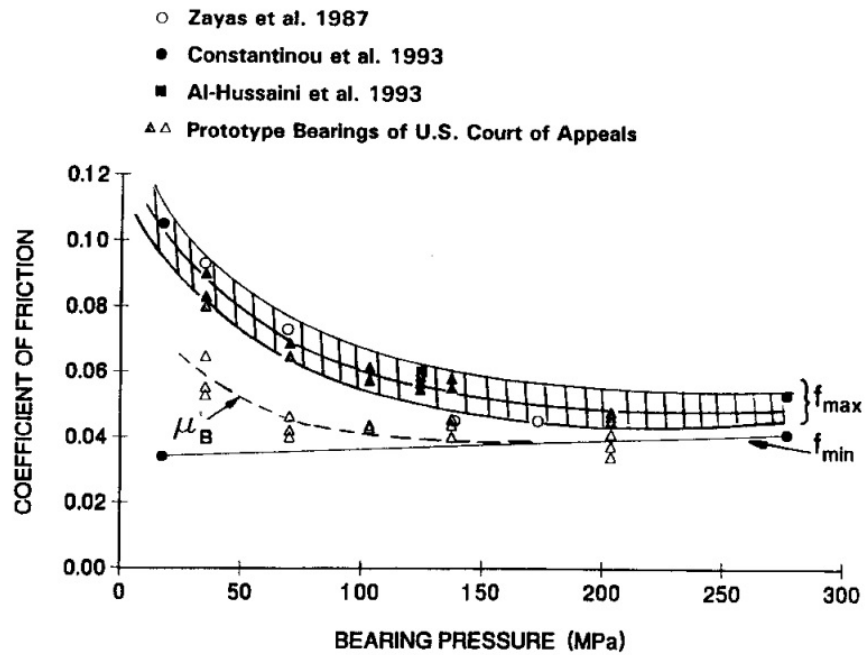


FIGURE 2.8: Frictional Properties of FPS Bearings

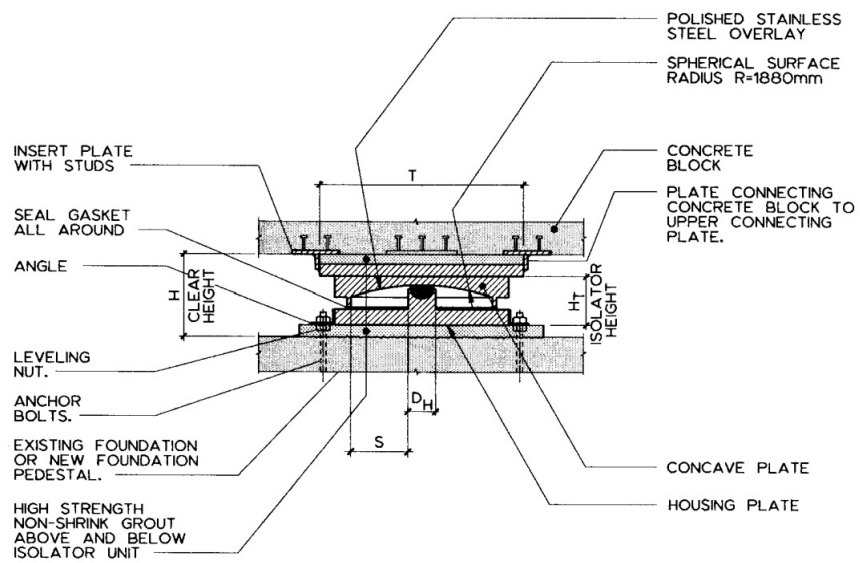


FIGURE 2.9: Cross Sectional View of FPS Bearings

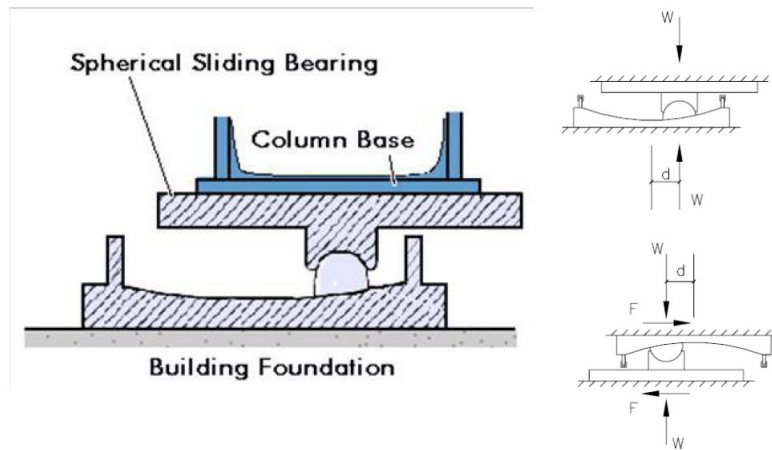


FIGURE 2.10: Friction Pendulum Sliding Isolator

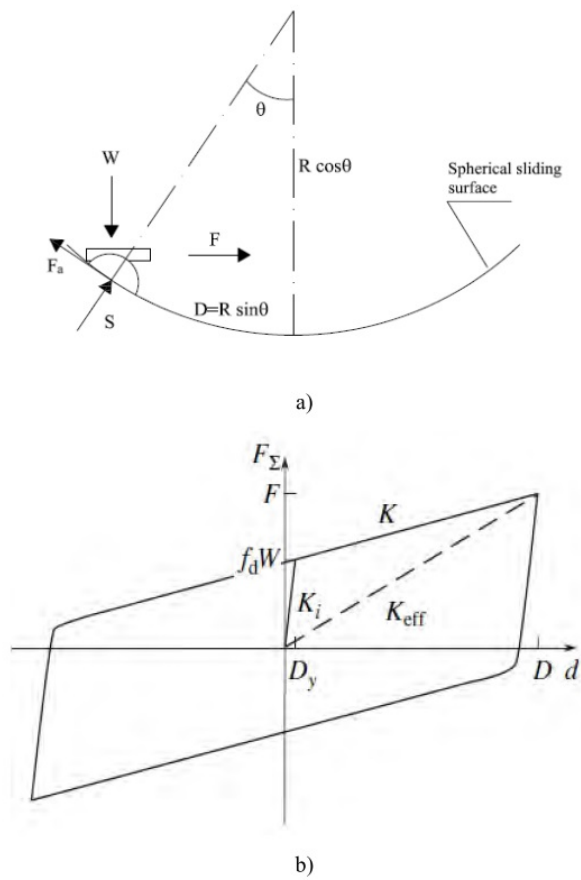


FIGURE 2.11: a) The mathematical model of the pendulum in the Equilibrium Phase
 b) Dynamical Characteristics of the FPS

the first pendulum isolator under expert supervision and guidance from the manufacturer's engineer. Dust, dirt, grit, mortar or any foreign matter must not be allowed to enter the moving parts. Therefore the FPS isolators should not be dismantled after leaving the manufacturer's workshop. Drawings should be checked against the project drawings with respect to the installation marks.

2.5.5.1 Acceptance of the Pendulum Bearings

After arrival on the site, the pendulum isolators must be checked via an acceptance procedure. First of all, the seismic isolator bearings, should be free of external visible damages, they must be clean and protected from corrosion damages. Furthermore, they must be tight temporary fixed and checked of working scale and value and direction if are pre-set by the manufacturer.

2.5.5.2 Storage

If the Pendulum Isolator Bearings are not installed upon delivery, they must be stored on wooden pallets at an appropriate place in the interim time. During storage, seismic isolators must be kept clean and protected from mechanical damages, moisture, excessive heat, sunlight, oils, fuels and other possible effects. In order to prevent condensation of water, air circulation must be ensured.

2.5.5.3 Placing and Adjusting

The construction company is required to provide all the appropriate tools, lifting equipment and if necessary scaffolding for the installation.

Elevation and direction of axes must be defined by the bridge design engineer. The axial directions are to be marked on the concrete substructure. The location drawing is the basis for setting out the Friction Pendulum Bearings in their correct position. It is very important, all the markings and adjustments to be observed.

X - and Y -axis are indicated on the lower and upper part of the friction pendulum isolator with center marks. Positioning has to be such that the center marks coincide with the axial directions marked on the superstructure.

The installation level and horizontal position are adjusted with shim plates. Small pendulum isolators are placed on the shim plates on the concrete surface of the substructure and should be fixed to the reinforcement with additional re-bars in order to prevent displacement during grouting¹.

2.5.5.4 Grouting (Mortar Bed)

The pendulum isolators shall be evenly supported over their entire area. Therefore, bedding surfaces must be flat and free from high points and hard spots. The thickness of the mortar bed is described in the construction drawings.

The choice of bedding material is influenced by the size of the gap to be filled, the size of the pendulum isolator, the strength required, access, and the required setting time. In some cases it may be necessary to carry out trials to ascertain the most suitable material particularly if flowable mortar is used.

After alignment, the temporary support of the pendulum isolator must remain in place until the mortar is properly set. The seismic isolator bearings have to be fixed properly in their required position, e.g. by welding of studs to the reinforcement. The recess spaces for the sockets or the shear connectors should be concreted before providing the mortar bed in order to avoid a local post-shrinkage in this area. The Seismic Isolators and the concrete of the substructure must be free of grease and oil.

If mortar gets on the pendulum isolators during the grouting procedure, it must be properly removed immediately.

2.5.5.5 Construction of Mortar Bed

For Seismic Isolation Bearings with sockets or shear connectors, flowable mortar or grouts are the best choice. The grout can be poured with a limp plastic hose and the aid of a funnel into the form.

Another and easier possibility is to use a half pipe instead of a hose with funnel. This requires more careful work in order to avoid spilling of grout onto the pendulum isolator. The procedure is expressed in Figure 2.12.

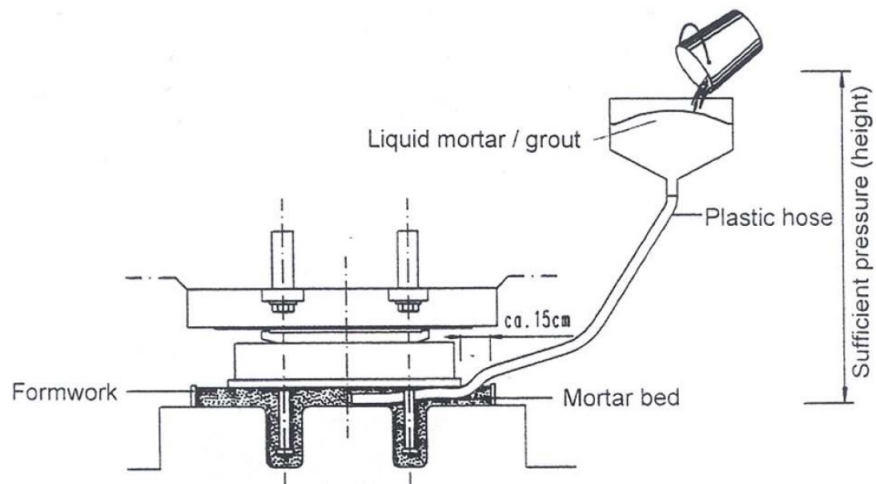


FIGURE 2.12: Construction and Installation of the Mortar Bed



FIGURE 2.13: Construction and Installation of the Mortar Bed using the free flow mortar

The most important part during the installation procedure is to de-aerate well, e.g. with metallic chains which are pulled back and forth. The distance between the chains shall be approx. 15 to 20 cm. The grout has to be poured until the gap is filled and about 1cm above the lower surface of the bottom plate.

¹Grouting is the proper unreinforced concrete that will fill the gap between the concrete substructure and bottom plate of the pendulum isolator

2.5.5.6 Concrete Superstructure

Generally the superstructure will be poured directly on the top plate of the pendulum isolator. The proper formwork has to be placed as close as possible to the top plate and the remaining gap has to be carefully sealed to ensure that no grout leaks onto the vertical face of the seismic isolator bearing. Sliding plates must be fully supported, to prevent tilting displacement or distortion of the isolator under the weight of wet concrete. After removal of the formwork, the seismic isolators have to be cleaned and any damage to corrosion protection must be repaired. These works must be done carefully in order to prevent any further damage.

Chapter 3

Friction Models

3.1 Introduction

Friction is a phenomenon when two physical surfaces are in contact and can be appear in different cases. For instance, friction appears when two solid elements are in contact and are sliding at different velocities.

This phenomenon is very usual in physics and in the engineering field. For example, in transmissions, in machines, in fluid mechanics. This phenomenon is non-linear, so it is of great importance to study the real frictional effect as accurately as possible. This can result in a reduction of errors consequential to the non-linear behaviour. In structural engineering, friction is used for energy dissipation. There are control devices that use friction to function and protecting at the same time structures from high seismic forces.

3.2 The phenomenon of Friction

Friction is a force that occurs between two surfaces in contact and acts in the opposite direction of the displacement. It depends on the properties of the materials in contact, the contact geometry, the velocity of the contact surfaces and the type of the contact involved. For instance lubricated or dry contact.// Figure 3.1 shows us the mechanism that is involved in a dry contact can be simplified as the contact between the micro-asperities of the material. Each micro-asperity carry a load, the summation of which will equilibrate the normal force N . The deformation of each asperity is elastic until the tangential load exceeds the shear strength of the material used. Then the deformation becomes plastic.

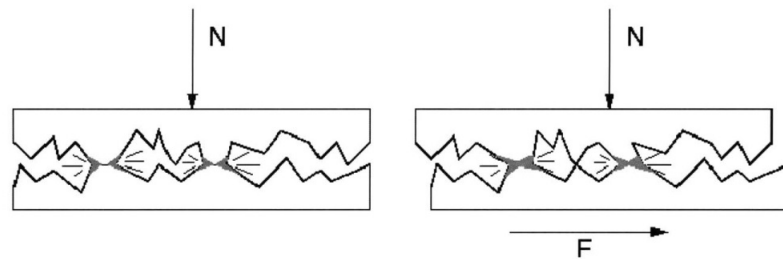


FIGURE 3.1: Simplification of the friction Phenomena

The classical rule for the friction phenomenon depends on the normal force N and the friction coefficient μ .

$$F = \mu N \quad (3.1)$$

There are two basic types of friction. The first is the static friction, that does not involve a motion of the two surfaces relatively to each other. The second type is the dynamic friction that involves the motion between the two surfaces. In each friction phase there is another μ . The coefficients μ_{static} and $\mu_{dynamic}$ respectively. In case of dry sliding the friction coefficient does not depend on the normal force N . In order to control the coefficient we need an extra interface between the two surfaces.

It is certainly more difficult to interpret the phenomenon of friction when between the two bodies exist some kind of lubricant, because it affects the phenomenon of friction. For low velocities and a low pressure distribution, friction depends on the shear forces in the fluid because of the hydrodynamic effects in the lubricant. These shear forces are related to the viscosity of the fluid and shear velocity. For high velocities and a high pressure distribution, the lubricant reacts as a solid. In high pressures the liquid acts as a solid while it is transferred from the liquid phase to the an amorphous solid phase. In this case, shear forces are not related to the shear velocity. So the it is way more difficult to evaluate the friction force[7]. For solid lubricants the shear strength of the lubricants decreases by an increase in velocity. Thus, the coefficient of friction decreases with increasing velocities. When the lubricant layer is thick enough to separate totally the two surfaces, the friction coefficient increases because the hydrodynamic effects become more significant. This effect is called the Stribeck effect. In general, it is difficult to model the friction phenomena. However, several models have been introduced for both static and dynamic friction and capture approximately all the parameters of friction.

3.3 Classical Static Models

There are many static friction models. Some of these models account for several aspects of the friction phenomenon and others are limited to the minimum aspects.

Friction depends on the velocity v and the contact area between two surfaces as described in the equation 3.2.

$$F_{Friction} = F \text{sign}(v) \quad (3.2)$$

3.3.1 Coulomb Friction

Coulomb friction is defined by the equation 3.1.

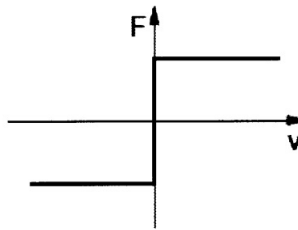


FIGURE 3.2: Coulomb Friction

Figure 3.2 shows the Coulomb friction. The value of the force for $v=0$ can be anywhere between $-F$ and $+F$.

3.3.2 Coulomb plus viscous friction

The phenomenon Coulomb plus viscous friction corresponds to the case where there is some lubricant between the two bodies that create friction. Viscous friction is described by the equation 3.3.

$$F = F_v v \quad (3.3)$$

Viscous friction is usually coupled with Coulomb friction. The resulting friction force is described in the equation 3.4.

$$F_{Friction} = F_v |v|^a \text{sign}(v) \quad (3.4)$$

This formulation provides a better approximation to the experimental data.

Figure 3.3 illustrates the profile of force vs. velocity in this type of friction phenomenon.

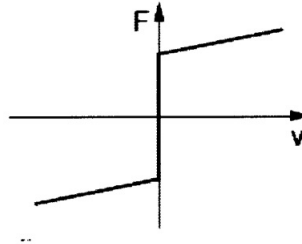


FIGURE 3.3: Coulomb plus Viscous Friction

3.3.3 Stiction plus Coulomb plus Viscous Friction

Stiction is shorter than in dynamic friction. Basically it is a force that counteracts the external forces and that is higher than the Coulomb force. The resulting friction force is described below.

$$F_{Friction} = \begin{cases} F_e & \text{if } v = 0 \text{ and } |F_e| < |F_s| \\ F_s \text{sign}(F_e) & \text{if } v = 0 \text{ and } |F_e| > |F_s| \end{cases} \quad (3.5)$$

where F_e represents the external force applied to the solid and F_s the stiction force.

When the velocity is null, the friction force depends on the external force. Thus, stiction can take any value between $-F_s$ and $+F_s$

The figure below (Fig. 3.4) shows the force vs. velocity profile of this type of friction.

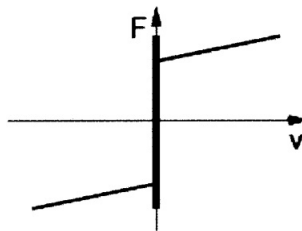


FIGURE 3.4: Stiction plus Coulomb plus Viscous Friction

3.3.4 Non-linearity: Stribeck effect

The last model that is the result of the observations made by Stribeck. The friction decreases continuously in terms of velocity dependence. The phenomenon is described below by the equation 3.6.

$$F_{Friction} = \begin{cases} F_v & \text{if } v \neq 0 \\ F_e & \text{if } v = 0 \text{ and } |F_e| < |F_s| \\ F_s \text{sign}(F_e) & \text{otherwise} \end{cases} \quad (3.6)$$

The F_v is commonly a function of the form

$$F(v) = F_c + (F_s - F_c)e^{-\left|\frac{v}{v_s}\right|^a} + F_v v \quad (3.7)$$

where F_c is the Coulomb friction force and F_s is the stiction force.

Figure 3.5 illustrates the non-linear phenomenon of the Stribeck effect.

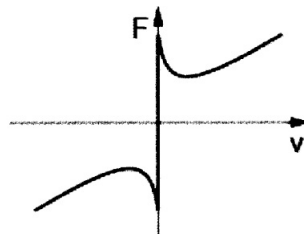


FIGURE 3.5: Stribeck Effect

The static models that we have seen before take into consideration only a part of friction characteristics. However, more precision is needed in the engineering applications in general. So, some dynamic models have been constructed in order to provide more accuracy in modelling friction. Besides that, numerical simulations are difficult to achieve with static models as sticking is difficult to distinguish from sliding.

3.4 Dynamic Models

3.4.1 The Dahl Model

The Dahl model is based on the stress-strain curve that is defined by the equation 3.8.

$$\frac{dF}{dx} = \sigma \left(1 - \frac{F}{F_c} \text{sign}(v)\right)^a \quad (3.8)$$

where v is the velocity, σ is the stiffness coefficient, F_c is the Coulomb force and a determines the shape of the stress-strain curve where is presented in Figure 3.6[8].

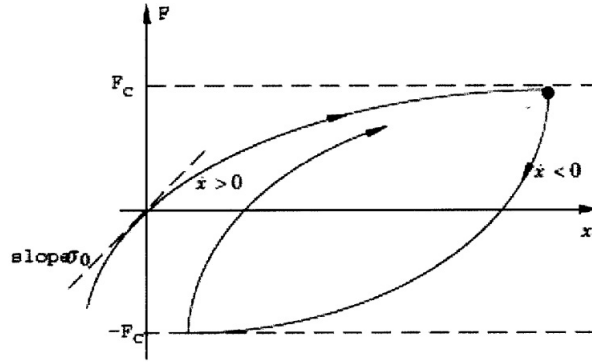


FIGURE 3.6: Friction Force vs. Displacement for the Dahl Model

In this case, the friction force is a function of the displacement. It is called rate independent, because it is dependent on the displacement and not on the velocity.[7],[8]. The stiction phenomenon and the Stribeck effect are rate dependent and the Dahl model cannot model these two phenomena.

A time domain model of the Dahl model can be obtained by

$$\frac{dF}{dt} = \frac{dF}{dx} \frac{dx}{dt} = \frac{dF}{dx} v = \sigma \left(1 - \frac{F}{F_c} \text{sign}(v)\right)^a \quad (3.9)$$

This model models neither the Stribeck effect nor the stiction phenomenon. It is the most general dynamic friction model because it is a generalization of the Coulomb friction phenomenon.

By setting the coefficient a equal to 1, the time domain equation becomes

$$\frac{dF}{dt} = \sigma \left(1 - \frac{F}{F_c} \text{sign}(v)\right) v \quad (3.10)$$

And by introducing the variable z such as $F = \sigma z$, the model can be written as in the equation 3.11.

$$\frac{dF}{dt} = v - \frac{\sigma |v|}{F_c} z \quad (3.11)$$

and Finally

$$F = \sigma z \quad (3.12)$$

3.4.2 The Bristle Model

This model has a very special characteristic. It tries to capture the frictional phenomenon at the microscopic scale. Moreover the irregularities of the surfaces that are in contact are the areas where friction happens. As the surfaces move relatively to each other, the bristles act like springs when in contact with the bonds. This creates friction force generated by the contact as shown in Figure 3.7.

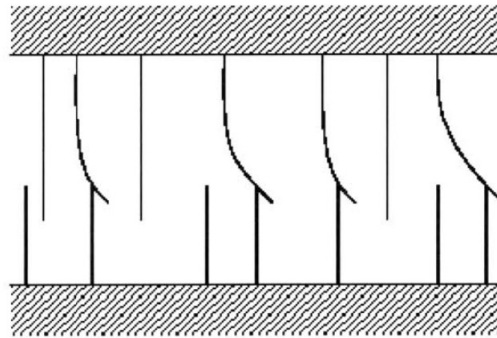


FIGURE 3.7: Asperities between two surfaces in contact

Essentially, the friction force is the sum of the forces created by each bristle. The friction that is created is given by the equation 3.13.

$$F = \sum_{t=1}^N \sigma_0 (x_t - b_t) \quad (3.13)$$

Where σ_0 is the stiffness of every bristle, x_t the position of the bristle and b_t the position of the bound. Thus, N is the number of the bristles and represents the number of contacts between the two bodies.

We have to admit that this model is very difficult for simulation as it is very complicated to know the number of the microscopic contacts between the two bodies. It needs a lot computational power and it is not efficient when N increases.

3.4.3 The LuGre Model

The concept of the LuGre model is nearly the same as the Dahl model except that the LuGre model can capture both the stiction and the Stribeck effect. It introduces an evolutionary variable that, for the LuGre model, corresponds to the bristle deflection (Figure 3.8). That is the reason why it is related to the Bristle model.

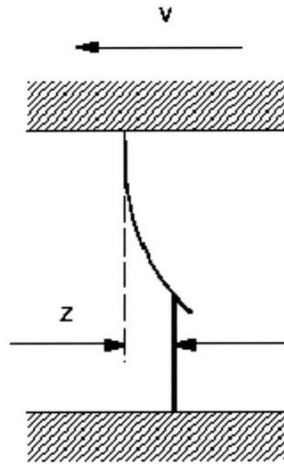


FIGURE 3.8: Evolutionary variable that corresponds to bristle deflection

The model is described by the following equations:

$$\frac{dz}{dt} = v - \sigma_0 \frac{|v|}{g(v)} z \quad (3.14)$$

$$F = \sigma_0 z + \sigma_1(v) \frac{dz}{dt} + f(v) \quad (3.15)$$

In equations 3.14 and 3.15, z represents the bristle deflection and v represents the velocity of sliding motion. The equation 3.15 corresponds to the equation of motion of the system. The variable σ_0 corresponds to the stiffness of the bristles, σ_1 corresponds to the damping and the function $f(v)$ describes the viscous damping, which is linearly proportional to the velocity and can be expressed by the equation 3.16.

$$f(v) = \sigma_2 v \quad (3.16)$$

The function $g(v)$ is a function that describes the Stribeck effect.

A reasonable function to describe the rate-dependent relationship of the Stribeck effect is equation 3.17.

$$g(v) = \alpha_0 + \alpha_1 e^{-\left(\frac{v}{v_s}\right)^2} \quad (3.17)$$

When the velocity is null,

$$g(v) = a_0 + a_1 \quad (3.18)$$

which corresponds to the stiction force.

When the velocity is high,

$$g(v) = a_0 \quad (3.19)$$

which corresponds to the Coulomb friction. Thus, the description for this model is the following:

$$\frac{dz}{dt} = v - \sigma_0 \frac{|v|}{g(v)} z \quad (3.20)$$

$$g(v) = \alpha_0 + \alpha_1 e^{-\left(\frac{v}{v_s}\right)^2} \quad (3.21)$$

$$F = \sigma_0 z + \sigma_1 \dot{z} + \sigma_2 v \quad (3.22)$$

3.4.4 The Leuven Model

This model is developed by Swevers and is a modified LuGre model. The difference lies within the pre-sliding stage, the behaviour being a hysteretic function $F_h(z)$ with nonlocal behaviour. For the sliding stage both Leuven and LuGre model share the same properties.

$$\frac{dz}{dt} = v \left(1 - \text{sign} \left(\frac{F_h(z)}{g(v)} \right) \left| \frac{F_h(z)}{g(v)} \right|^a \right) \quad (3.23)$$

$$g(v) = (F_s - F_c) e^{-\left| \frac{v}{v_s} \right|^2} \quad (3.24)$$

$$F_f = F_h(z) + \sigma_1 \frac{dz}{dt} + \sigma_2 v \quad (3.25)$$

3.5 Friction Damping

Coulomb damping is characterized by damping force that is in phase with the deformation rate and has constant magnitude. The force can be expressed as follows:

$$F = \bar{F} \operatorname{sgn}(\dot{u}) \quad (3.26)$$

Figure 3.9 shows the variation of F with u for periodic excitation. The work per cycle is the area enclosed by the response curve.

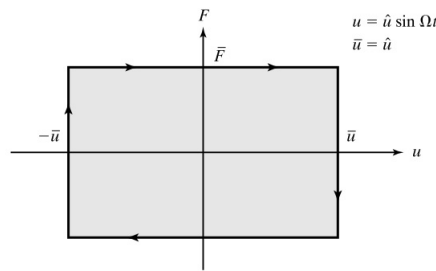


FIGURE 3.9: Coulomb damping Force vs Displacement

$$W_{Coulomb} = 4\bar{F}\bar{u} \quad (3.27)$$

Structural damping removes the restriction on the magnitude of the damping force to be proportional to the displacement amplitude. The definition equation for this friction model has the form:

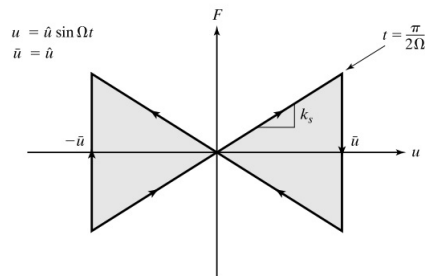


FIGURE 3.10: Structural damping Force vs Displacement

$$F = k_s |u| \operatorname{sgn}(\dot{u}) \quad (3.28)$$

where k_s is a pseudo-stiffness factor. The energy dissipated per cycle is equal to

$$W_{structural} = 4 \left(\frac{k_s \bar{u}^2}{2} \right) = 2k_s \bar{u}^2 \quad (3.29)$$

Chapter 4

Non Linear Dynamic Analysis Procedure

Nonlinear dynamic time-history analysis was performed to evaluate the performance of the isolation system and superstructure for the FPS isolation system design. The system comprises a five storey building with base isolation. The system that isolates the building is a friction pendulum isolator system. The floors have their own stiffness k_c and the friction pendulum isolator has its own stiffness k_r , which depends on the radius of curvature and the mass of the structure bearing down on that particular sliding surface. The important acknowledgement in this thesis is that the system constructed models the entire floor or ceiling as the sliding surface, rather than just the sliding surface that exists between two FPS isolators.

The main concept is to isolate the building from its base and reduce the relative motion and absolute motion of each floor and the shear forces during a seismic event. The principle is to make the structure more flexible.

4.1 Modelling and Analysis Details

For the purposes of the system modelling a five-story reinforced structure (Figure 4.1) is used and modelled as a mass, spring-damper model.

The equation of motion is the following.

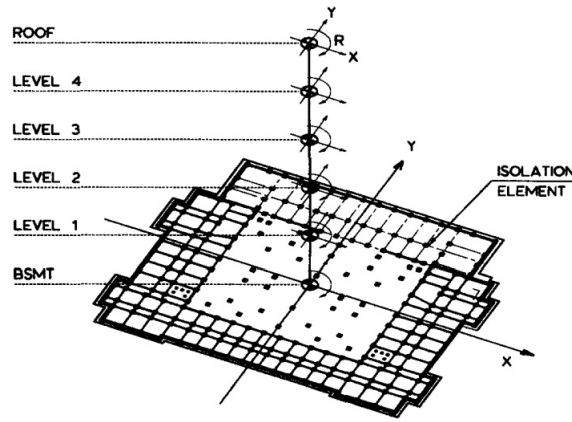


FIGURE 4.1: Model for dynamic analysis

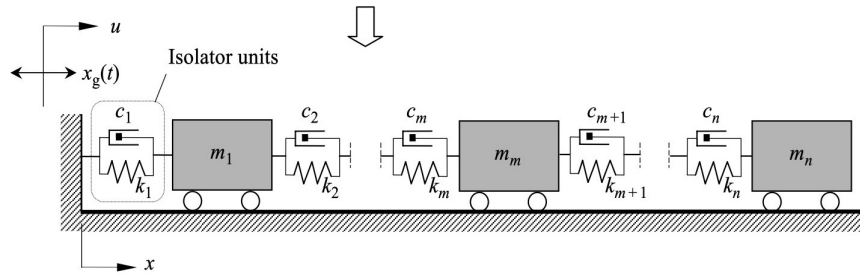


FIGURE 4.2: System modelled in Matlab

$$m\ddot{u}_m + k_{cm}(u_m - u_{m-1}) + c_m(\dot{u}_m - \dot{u}_{m-1}) - k_{cm+1}(u_{m+1} - u_m) - c_{m+1}(\dot{u}_{m+1} - \dot{u}_m) = -m\ddot{u}_g \quad (4.1)$$

In matrix form:

$$M\ddot{U} + C\dot{U} + KU = -M\ddot{U}_g \quad (4.2)$$

Where C is the damping matrix of the structure and according to the equation 4.3 is taken as proportional to the stiffness of the structure by the constant a[9].

$$C = aK \quad (4.3)$$

Where a is a positive scalar and is expressed by the equation 4.4.

$$\xi = \frac{a\omega}{2} \quad (4.4)$$

Where ξ is the damping ratio is assumed equal to 0.02.

The stiffness of the floors were calculated as follows[9].

$$S\dot{k} = M\Phi \quad (4.5)$$

$$K = \omega^2\dot{k} \quad (4.6)$$

Where Φ is the mode shape that describes the desired displacement profile.

These Equations were assigned into a Simulink Model using a State-Space function(See Appendix). An unscaled Earthquake excitation was downloaded from the PEER Ground Motion Database and then scaled in an upper bound of 0.12 g by a Gain block and plugged into Simulink Model. Two models were constructed. One uncontrolled that takes into consideration the structure without the FPS Bearings on it's base and was used as reference to which the controlled structure would later be compared. The main idea was to decrease the acceleration and the inter-story displacement of the structure. An extra stiffness parameter k_r was included on the base of the structure which corresponds to the stiffness of the Friction Pendulum System.

$$k_r = \frac{nmg}{R} \quad (4.7)$$

Where:

n = Number of stories above the FPS isolator Bearing

m = Storey mass

R = Radius of Curvature

For a given FPS, mass in the equation 4.7 is total mass of the stories above that point. The Radius R was taken to be equal to 100 m according to the bibliography which corresponds to a deflection of 0.3 m at mid-span of the floor. Besides that, the friction phenomenon which exists between the two curved plates of the isolator during the earthquake excitation must be included in the model. This is expressed as:

$$F_r = \mu mg \quad (4.8)$$

Where:

μ = Coefficient of Friction

m = Mass

g = Acceleration of gravity

The Force that was plugged in the Matlab Simulink Model is expressed as:

$$F = k_r u + (\mu m g) \text{sign}(\dot{u}) \quad (4.9)$$

4.2 The Concept of Base Isolation

The main concept of base isolation systems is to interpose structural elements with low horizontal stiffness between the structure and the foundation in order to decouple the structure from the horizontal ground motion which gives the structure a very low frequency than both its fixed base and the ground excitation. The deformation of the first dynamic mode happens in base isolation while the structure above is rigid. The deformation of higher modes happens in the structure which is orthogonal to the first mode and to the ground motion. These higher modes do not participate in the motion. Therefore the high energy in the ground motion cannot be transmitted to the structure. It is clear that the base isolation system does not absorb the energy from an earthquake excitation but it deflects it through the system dynamics which is not depending on the damping level. Dampers are important to suppress resonance at the isolation frequency.

4.2.1 Effectiveness of base isolation

The main function of the base isolation is to reduce the base shear, for this purpose the period ratio T_b/T_f should be large as practical, otherwise it will be harmful. For instance, during 1985 in Mexico City the earthquake excitation that occurred in a one-storey building with pseudo-acceleration value $A(T_f, \zeta_f) = 0.25g$ associated with $T_f = 0.4\text{sec}$ and $\zeta_b = 10$ for the isolated structure. The ratio $A(T_b, \zeta_b)/(T_f, \zeta_f) = 0.63g/0.25g = 2.52$ means that the base shear in the base-isolated building is 2.52 times the base shear in the fixed-base building as $T_b \gg f$.

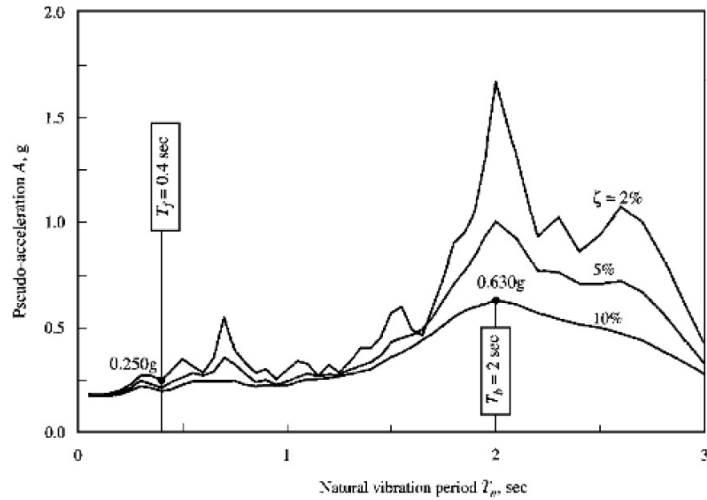


FIGURE 4.3: Response spectrum for ground motion recorder on Sep 19,1985 at SCT site on Mexico City and spectral ordinates for fixed-base and isolated building

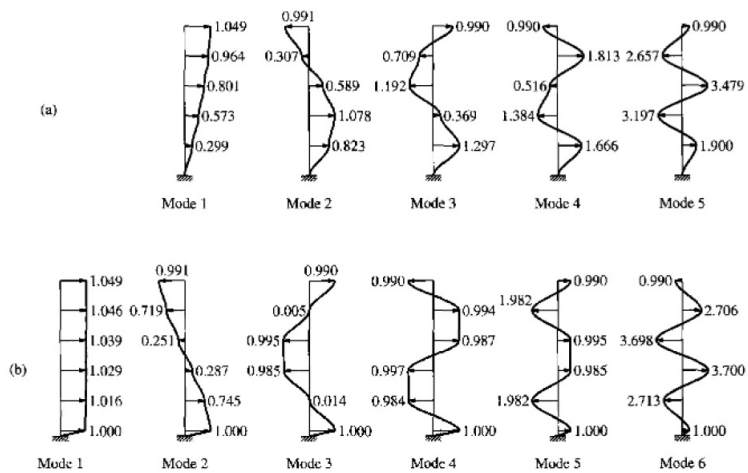


FIGURE 4.4: Natural Vibration Models

Chapter 5

Results

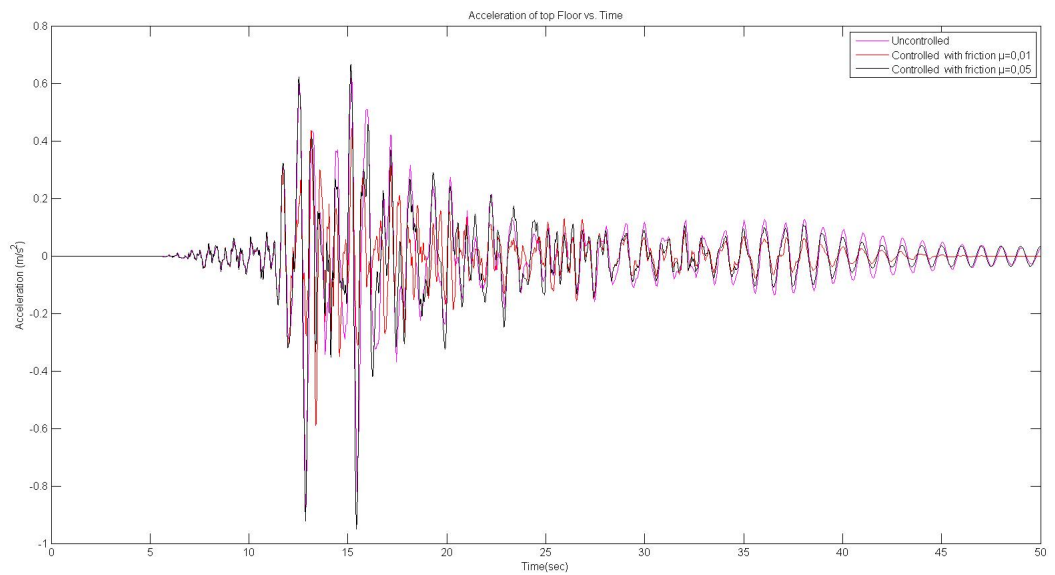


FIGURE 5.1: Acceleration of Top Floor VS Time

The Figure 5.1 presents the acceleration of the top floor in general. The magenta graph describes the uncontrolled system and the black and blue graphs describe the controlled system with the inclusion of friction. Obviously with the presence of the FPS isolation bearing the acceleration of top floor has been significantly reduced. But by increasing the friction coefficient to 0.05, the acceleration increases slightly.

Figure 5.2 presents the displacement of top floor vs time. The displacement is significantly reduced with the interaction of the FPS isolation bearing.

Figure 5.3 presents the upper and lower Slab accelerations versus time. The blue graph describes the uncontrolled system and the green graph the controlled system with the

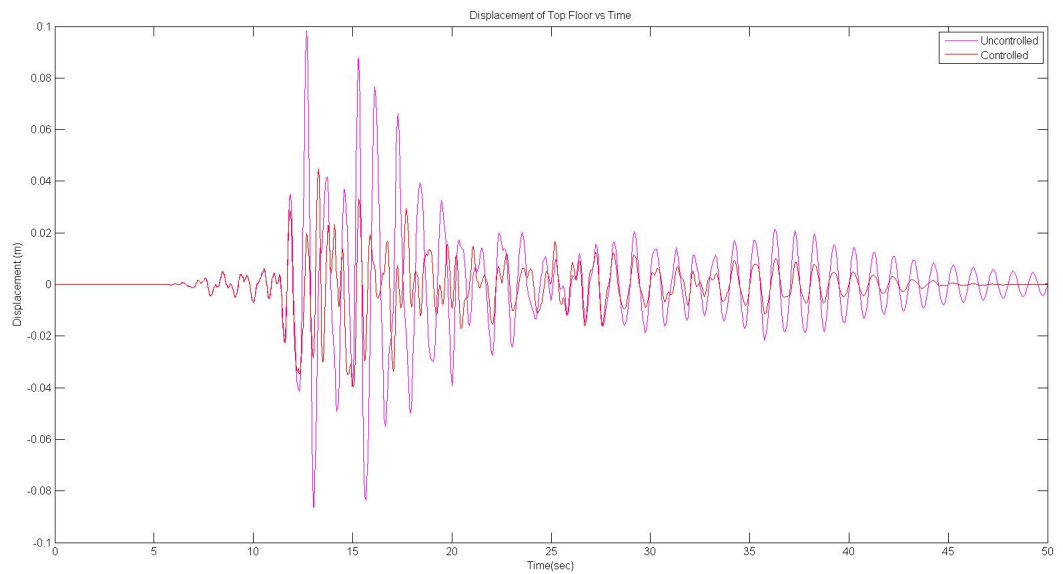


FIGURE 5.2: Displacement of Top Floor VS Time

presence of the FPS isolator. The inter-slab accelerations will be higher because of the elastic effect of the FPS system. On the contrary, near the slab of the fixed base structure, smaller accelerations may occur.

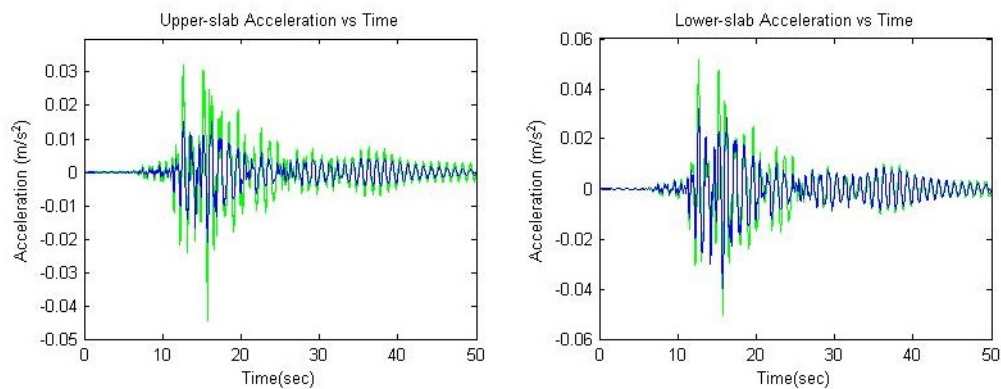


FIGURE 5.3: Upper and Lower Slab Accelerations VS Time

Figure 5.4 presents the Hysteretic Behaviour of the friction forces that occur in the sliding mechanism of the FPS system during a seismic event. According to the chapter (3.3.1) the cyclic event of the friction force as shown in Figure 5.4 can be confirmed by the Figure 3.2 which illustrates the profile of friction force vs velocity during the friction phenomenon.

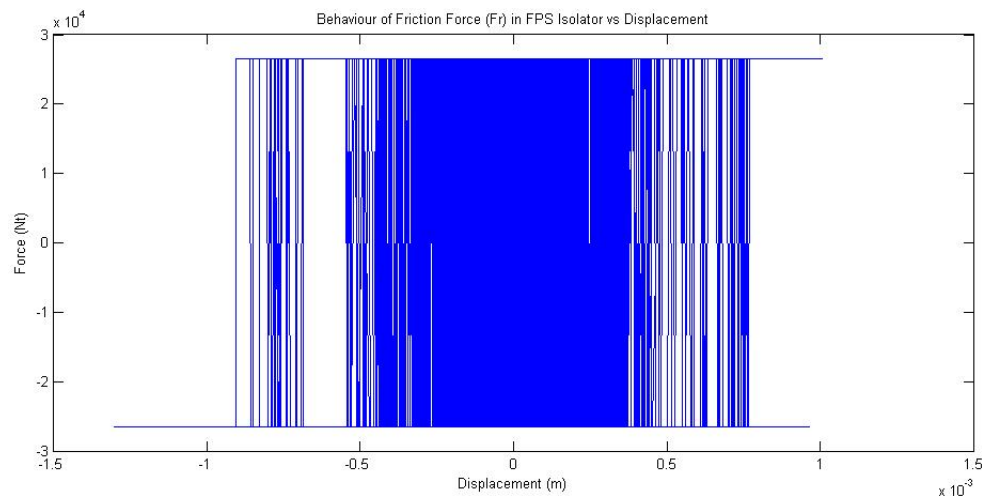


FIGURE 5.4: Behaviour of Friction Forces (Fr) vs Displacement

Chapter 6

Conclusions

6.1 Conclusions

The research that accomplished in this thesis shows that Friction Pendulum System Bearings implemented as seismic isolation devices on the base of a structure could be an effective mechanism of damping seismic forces that occur in a structure during a seismic event. The simulation that has been done in this thesis took into consideration a structure with the presence of FPS isolation Bearings in its base and one without any base isolation. Both structural schemes subjected on an earthquake excitation and the difference in responses of both models was calculated by comparing these two scenarios. Results have shown that the success of the FPS base isolation devices is strongly dependent on the friction coefficient during the friction phenomenon that occur between the sliding surfaces. Higher friction forces cause the columns above to absorb a higher amount of seismic forces. However, by the carefully selecting the amount of friction between the sliding surfaces, energy could be dissipated while transferring less to the upper floors. The results show that the displacement of top floor is less with the lower friction coefficient due to the fact that the floor system can dissipate more freely. this effect is more safe as less forces are transferred into the upper parts of the building and less shear forces occur during the seismic event. Overall the FPS isolation system showed a significant improvement in dynamic response of the model structure by reducing the lateral acceleration and increasing the damping of the system. However the conventional isolation systems using pure friction and friction pendulum system have many limitations, and are effective only for certain structural and excitation parameters.

There are some issues of the FPS isolation system that should be considered for its implementation. In practice, flexible mechanical components should be considered in the main construction plan. Such as seismic isolation components for pumping or HVAC

systems. Another ceiling mechanisms should be installed and considered in the main drawings of the structure such as elastic devices in the staircases, elevators and safety gaps that will give the ability to the structure to dissipate freely without being damaged. In addition FPS base isolation Bearings are expensive and the peripheral ceiling mechanisms that mitigate the shear forces which occur during an earthquake event increase the cost of a structure.

In the Future, further studies should include tests of stronger earthquakes as well as harmonic excitations to assess the behaviour of individual structures. Further research should focus on the development of more efficient systems that can provide stiffness between the levels of discontinuity. Furthermore, mass production of FPS seismic isolation system would have a positive impact in smaller scale structures that are located in places where continuous seismic events occur.

Appendix A

MATLAB Simulink Models

The following graphs show the uncontrolled and controlled models that constructed to simulate the structure.

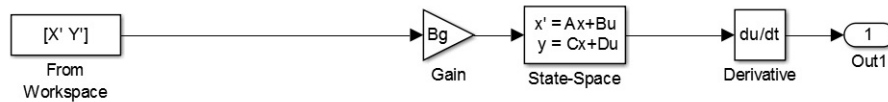


FIGURE A.1: Uncontrolled Simulink Model

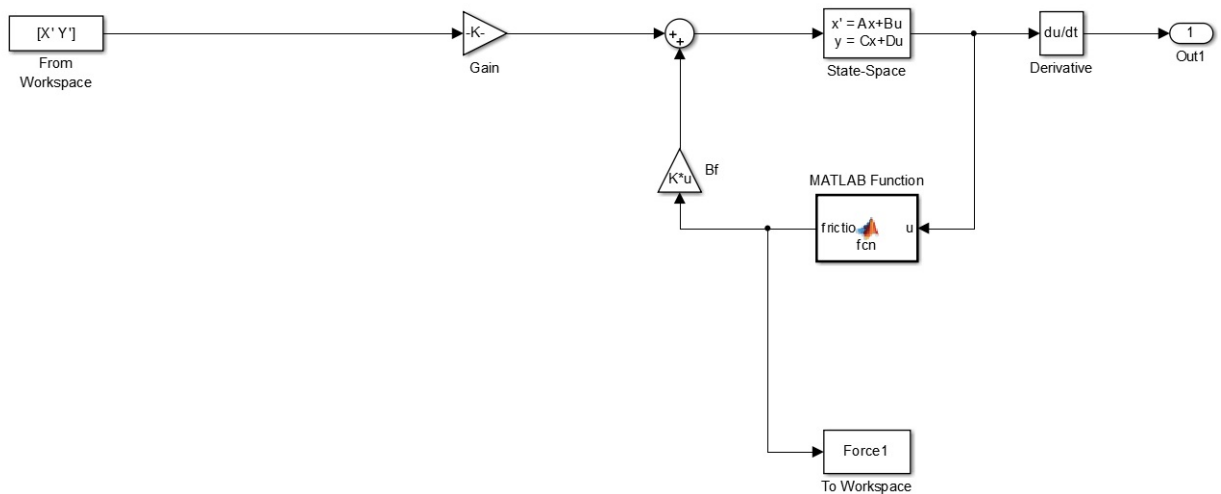


FIGURE A.2: Controlled Simulink Model with the Inclusion of Friction

Appendix B

State Space Formulation

The dynamic response of the SDOF linear system shown in Fig B.1 is governed by the second-order equation[9]

$$m\ddot{u} + c\dot{u} + ku = -ma_g + p + F \quad (\text{B.1})$$

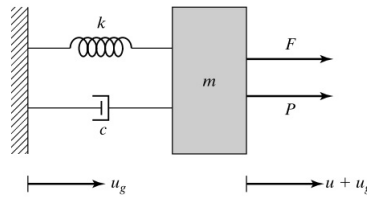


FIGURE B.1: SDOF System.

where p is the applied external loading, F is the active Force, and m, k, c are constant system parameters. Integrating Eq.(B.1) in the time and enforcing the initial conditions on u and \dot{u} at $t=0$, we obtain the velocity and displacement as functions of time. These quantities characterize the state of the system. Acceleration and internal forces can be determined by backsubstitution.

It is more convenient to work with a set of first order equations rather than with a second-order equation.

$$\frac{du}{dt} = \dot{u} \quad (\text{B.2})$$

$$\frac{d\dot{u}}{dt} = \left(-\frac{c}{m}\right)\dot{u} + \left(-\frac{k}{m}\right)u + (-1)a_g + \left(\frac{1}{m}\right)p + \left(\frac{1}{m}\right)F \quad (\text{B.3})$$

This form is called state-space representation. By this form complexity in generating both analytical and numerical simulations can be reduced. Defining \mathbf{X} as the state vector,

$$\mathbf{X} = \begin{bmatrix} u \\ \dot{u} \end{bmatrix} = \mathbf{X}(t) \quad (\text{B.4})$$

the matrix equilibrium equation is written as

$$\frac{d\mathbf{X}}{dt} = \dot{\mathbf{X}} = \mathbf{A}\mathbf{X} + \mathbf{B}_f F + \mathbf{B}_g a_g + \mathbf{B}_p p \quad (\text{B.5})$$

where the various constant coefficient matrices are defined as follows:

$$\mathbf{A} = \begin{bmatrix} 0 & 1 \\ -\frac{k}{m} & -\frac{c}{m} \end{bmatrix} \quad (\text{B.6})$$

$$\mathbf{B}_f = \mathbf{B}_p = \begin{bmatrix} 0 \\ \frac{1}{m} \end{bmatrix} \quad (\text{B.7})$$

$$\mathbf{B}_g = \begin{bmatrix} 0 \\ -1 \end{bmatrix} \quad (\text{B.8})$$

The initial condition at $t=0$ are denoted by \mathbf{X}_0 .

$$\mathbf{X}(0) = \begin{bmatrix} u(0) \\ \dot{u}(0) \end{bmatrix} \equiv \mathbf{X}_0 \quad (\text{B.9})$$

With this representation, the problem is reduced to solving a first order equation involving \mathbf{X} .

The equations for an n th order linear system subjected too seismic excitation and a set of control forces applied at various locations on the system are written as^[9]:

$$M\ddot{\mathbf{U}} + C\dot{\mathbf{U}} + K\mathbf{U} = -MEa_g + E_f F + P \quad (\text{B.10})$$

where E_f is an $n \times r$ matrix that defines the location of the control forces with respect to the degrees of freedom. The initial condition involve constraints on the displacement

and velocities at time $t = 0$.

$$\mathbf{U}(0) = \mathbf{U}_0 \quad (\text{B.11})$$

$$\dot{\mathbf{U}}(0) = \dot{\mathbf{U}}_0 \quad (\text{B.12})$$

So the state - space form is taken as:

$$\dot{\mathbf{X}} = \mathbf{A}\mathbf{X} + \mathbf{B}_f\mathbf{F} + \mathbf{B}_g a_g + \mathbf{B}_p \mathbf{P} \quad (\text{B.13})$$

where \mathbf{X} is a vector of $2n$ order.

and the coefficient matrices are given by

$$\mathbf{A} = \begin{bmatrix} \mathbf{O} & \mathbf{I} \\ -\mathbf{M}^{-1}\mathbf{K} & -\mathbf{M}^{-1}\mathbf{C} \end{bmatrix} (2n \times 2n) \quad (\text{B.14})$$

$$\mathbf{B}_f = \begin{bmatrix} \mathbf{O} \\ \mathbf{M}^{-1}\mathbf{E}_f \end{bmatrix} (2n \times r) \quad (\text{B.15})$$

$$\mathbf{B}_g = \begin{bmatrix} \mathbf{O} \\ -\mathbf{E} \end{bmatrix} (2n \times 1) \quad (\text{B.16})$$

$$\mathbf{B}_p = \begin{bmatrix} \mathbf{O} \\ \mathbf{M}^{-1} \end{bmatrix} (2n \times 1) \quad (\text{B.17})$$

Bibliography

- [1] Mahmoud Sayed-ahmed. Building with base isolation techniques. *Journal of Al-Azhar University Engineering Sector (JAUES)*, 7(1):147–159, December 2012.
- [2] Iemura H, Jain SK, and Pradono MH. Seismic base isolation and vibration control. *Chapter 29 of the Vibration and Shock Handbook*, Editor in Chief, C.W. de Silva, CRC Press, Taylor and Francis Group, LLC, 2005.
- [3] Buckle I and Mayes R. Seismic isolation: history,application and performance a world overview. *Earthquake Spectra*, 6(2):161–202, December 1990.
- [4] F. Naeim and J. M. Kelly. *Design of Seismic Isolated Structures: From Theory to Practice.*, chapter 1. John Wiley & Sons, Inc., 1999.
- [5] Zayas V.A, Low S.S, and Mahin S.A. A simple pendulum technique for achieving seismic isolation. *Earthquake Spectra*, (6):317–333, 1990.
- [6] Fraklin Y. Cheng, Hongping Jiang, and Kangyu Lou. *Smart structures: innovative systems for seismic response control*, chapter 2. Taylor & Francis Group, 2008.
- [7] Olsson H, Astrom K.J, Canudas De Wit C., Gafvert M., and Lischinsky P. Friction models and friction compensation. *European Journal of Control*, 4:176–195, 1998.
- [8] Dahl P. A solid friction model, technical report tor-0158h3107-181-1. *The Aerospace Corporation, El Segundo, CA*, 1968.
- [9] Jerome J. Connor. *Introduction to Structural motion control*, chapter 5. Pearson Education, Inc Upper Saddle River,New Jersey 07458, 2003.